Strain and composition in SiGe nanoscale islands studied by x-ray scattering

Th. Wiebach, M. Schmidbauer, M. Hanke, H. Raidt, and R. Köhler
AG Röntgenbeugung, Institut für Physik, Humboldt-Universität zu Berlin, Hausvogteiplatz 5-7, D-10117 Berlin, Germany

H. Wawra
Institut für Kristallzüchtung, Rudower Chaussee 6, D-12489 Berlin, Germany
(Received 7 September 1999)

High-resolution x-ray diffraction has been performed on strained SiGe nanoscale islands grown coherently on Si(001). Reciprocal space maps show a widely extended ''butterfly''-shaped island reflection and strong diffuse scattering around the substrate reflection. From such intensity maps the Ge content and its distribution inside the islands are evaluated. This is done by simulation of diffuse scattering for a variety of island models. The island shape is known from atomic force and scanning electron microscopy. The only free parameter was the Ge distribution, here approximated by a vertical concentration profile. With an abrupt increase of Ge content at about one third of the island height a rather good agreement with the experimental results is achieved. The strain distribution in the islands is then given by the finite element calculations, which are part of the simulation algorithm.

I. INTRODUCTION

The development of low-dimensional nanoscale structures as novel electronic devices is presently among the most exciting challenges in semiconductor technology. In the recent past years self-organizing epitaxial growth mechanisms such as the Stranski-Krastanov growth mode[1] have been utilized for the generation of strongly strained coherent quantum dots.[2] The key parameters in such systems are size, shape, strains, and strain distribution since these quantities are decisively related to the electronic and optical properties. As, on the other hand, the Stranski-Krastanov mechanism is driven by strain a detailed characterization of morphology and strain distribution is crucial for a complete understanding and control of the growth process. Despite this there is still no satisfactory knowledge about these properties and their mutual interaction. Moreover, in alloys, decomposition may occur during or after growth. Tersoff[3] has theoretically predicted that strain-induced segregation drastically increases the nucleation rate. This may lead to a composition gradient inside the islands.

A powerful technique of strain determination is the evaluation of atomic displacement vectors through the quantitative analysis of high-resolution transmission electron micrographs (see, e.g., Ref. 4). However, beside the serious problem in defining an appropriate reference lattice the accuracy of strain values is in the range of 10^{-3} (see, e.g., Ref. 5). Furthermore, the results are in first approximation an average over the foil thickness and certainly sensitive to foil warpage and three-dimensional strain relaxation in the foil. Also, only single quantum dots can be investigated so that the measured displacement vectors often suffer from missing statistics.

X-ray scattering has been successfully applied to the characterization of strain[6–11] and morphology[10,12–14] of nanoscale islands. A direct reconstruction of morphology, strain, and composition from the diffraction pattern is, however, not possible. The systems considered here are complicated since the strain tensor components ε_{ij} depend on all three space coordinates x,y,z. Therefore, up to now simulations of x-ray intensities were based on simplified analytical approaches for the strain field: Steinfort *et al.*[6] performed an x-ray crystal truncation rod analysis on faceted Ge hut clusters grown on Si(001). They calculated diffraction profiles by using an empirical power law for the strain field. Moreover, they did not include the influence of the strain field on the underlying wetting layer and substrate, which is known to be considerably strong.[15] Darhuber *et al.* approximated the long range field of elastic relaxation in multiple layers of Ge islands in Si(001)[7] and of $In_xGa_{1-x}As$ quantum dots in GaAs,[8] respectively, by the deformation field of anisotropic point defects. Kegel *et al.*[9] applied the concept of ''iso-strain scattering'' on the evaluation of strain in coherent InAs islands. This concept assumes that the effective strain is constant within layers parallel to the surface, which is at variance with calculations [see Fig. 3(c)] based on the finite element method (FEM).

In the present paper, a numerical ''brute-force'' method combined with high-resolution x-ray diffraction is introduced that allows for both the determination of the strain field and the composition in nanoscale islands. The basic idea of this approach is the calculation of the strain field by using the finite element method based on elasticity theory. Assuming well defined values of shape, size and composition, the elastic strain field $\mathbf{u}(\mathbf{r})$ can be calculated at each selected position inside the mesoscopic structure. In a second step, $\mathbf{u}(\mathbf{r})$ is used to simulate the x-ray scattering intensity. Since the mesoscopic structures are smaller than the x-ray extinction length kinematical scattering theory can be used as a good approximation. Recently, a similar concept of combining FEM and the calculation of x-ray diffraction has been applied to etched quantum wires.[16,17] An interesting alternative has been performed by Grundmann and Krost.[18] In the framework of the valence force-field model[19] they calculated the deformation field in InAs quantum dots buried in GaAs and subsequently simulated x-ray diffraction intensity profiles.

In order to quantitatively prove the validity of our approach a single layer of highly regular dislocation-free $Si_{0.75}Ge_{0.25}$ islands has been chosen that is coherently grown on Si(001) by means of liquid phase epitaxy (LPE). Since at LPE the driving forces are very low growth is carried out close to thermodynamical equilibrium, and the most relevant parameters that are influencing the growth process are the strain field within the island and the surface free energy.

The aim of this paper is to demonstrate the capability of our method of performing a full strain analysis of nanoscale islands which, in addition, includes the capability to determine a composition gradient inside the islands. We also would like to discuss selected features of the diffraction pattern and how they are influenced by the strain field. Direct attention is focused on the interplay of shape (size) and strain, which is substantial with regard to very small objects such as quantum dots.

In the next sections, the LPE sample preparation and the experiment are presented. Then, in Sec. IV, we describe how the finite element method is incorporated in x-ray diffraction simulations. In Sec. V, the experimental and simulated results are discussed. Finally, the conclusions are presented in Sec. VI.

II. SAMPLE PREPARATION

The sample preparation has been described in a previous paper in detail.[13] Briefly, the $Si_{1-c}Ge_c$ islands have been grown by liquid phase epitaxy (LPE) using a Bi solution. The epitaxial layers are deposited in a horizontal solution growth system that is kept under pure hydrogen. In order to ensure that the system is in thermodynamical equilibrium before growth starts the solution is homogenized at the growth temperature (973 K) for several hours. A low cooling rate of about 10 K/h has been chosen such that a low growth rate is achieved.

We have chosen a nominal Ge atomic fraction of $c = 25\%$. Monodisperse coherent islands are obtained in accordance to the observed relationship[20] $w \propto c^{-2.03}$ between the island base width w and the Ge concentration c. The surface morphology was investigated by atomic force microscopy (AFM) and scanning electron microscopy (SEM) such that the exact shape and size of the islands could be determined with high accuracy. The SiGe islands are of truncated pyramidal shape and are bounded by {111} side facets (Fig. 1). The island size distribution is rather narrow (10% full width at half maximum) with mean values of 135 and 80 nm for the island base width and the island height, respectively.

III. EXPERIMENT

High-resolution x-ray diffraction was performed at the BW2 wiggler station of HASYLAB/DESY with the use of monochromatic synchrotron radiation at $\lambda = 1.54\,\text{Å}$ and a relative bandwidth of about $\Delta\lambda/\lambda = 10^{-4}$. Figure 2 shows a schematic view of the scattering geometry. The vertical and horizontal spot size at the sample was typically 0.5 mm $\times$2 mm along with beam divergences within and perpendicular to the scattering plane of 0.05 and 0.2 mrad, respectively. A linear position sensitive detector (PSD) with a spatial resolution of about 80 μm has been placed 800 mm behind the sample such that different scattering angles 2Θ with respect to the incoming beam belong to different channels of the PSD. The PSD, therefore, acts as analyser of the scattered beam direction with a typical resolution of $\Delta q/q = 5 \times 10^{-4}$. This value is sufficiently small to ensure that all relevant diffraction features originating from the strained layer can be resolved. By rocking either the sample (ω scan) or, alternatively, both sample and PSD in 1:2 coupling ($\omega - 2\Theta$ scan) a complete two-dimensional map of reciprocal space can be measured in a single scan.[21] As our simulations will show the shape of diffuse intensity in these two dimensions is a characteristic ''fingerprint'' of the Ge distribution and, in that, is superior to single one-dimensional scans.

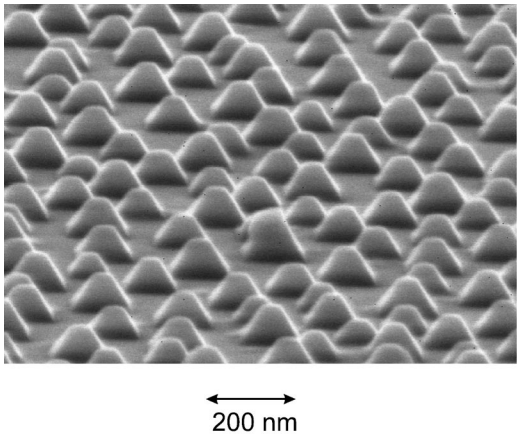

FIG. 1. Scanning electron micrograph of a $Si_{0.75}Ge_{0.25}/Si(001)$ layer. The sample consists of coherently strained truncated pyramids exhibiting {111} side facets and a (001) top facet. The island base width and height are about 135 and 80 nm, respectively, with a narrow size distribution.

Nearly the entire beam path between sample and PSD was evacuated by using a flight tube in order to ensure that strong air scattering is avoided. Slits of widths 2 mm have been placed at both ends of the flight tube. Consequently, in the direction perpendicular to the scattering plane we integrate over a distance of typically $\Delta q_y = 0.01\,\text{Å}^{-1}$. This value has been included in the calculations described below.

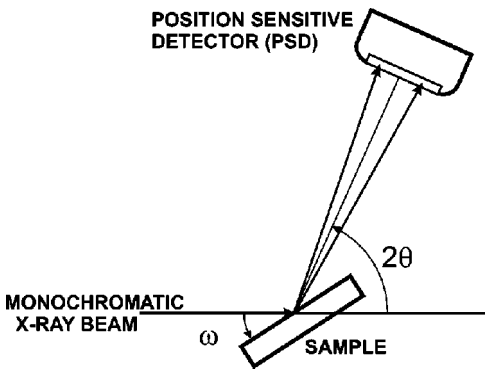

FIG. 2. Schematic view scattering geometry used in our experiment. The position sensitive detector (PSD) lies in the scattering plane, such that different angles 2Θ correspond to different channels. Note that, in the case of the $\overline{113}$ asymmetrical case (steep incidence and glancing exit) the scattering beam is highly compressed.

Although not restricted to these cases we have investigated the symmetrical 004 and the asymmetrical $\bar{1}13$ lattice points (steep incidence and glancing exit).

IV. THEORY

The parameters used in the FEM calculations (with the program package MARC) are the shape and size of a single island, the atomic Ge concentration c, the corresponding lattice parameter and the linear elastic moduli c_{ijkl} for cubic $Si_{1-c}Ge_c$. Shape and size of the island are known from other experiments[13,14] (AFM, SEM, and grazing incidence small angle scattering). In order to keep computation time in reasonable limits the Ge distribution was approximated by a one-dimensional (layered) vertical profile. This profile is the only free parameter. The corresponding lattice parameter and the linear elastic moduli are calculated by Vegard's law[22] (the small deviation of the lattice parameter from Vegard's law is less than the current accuracy of our calculations). The wetting layer thickness has been assumed as $d_{WL}=2$ nm. In agreement with previous work,[15] our calculations show that the strain field of the islands strongly penetrates into the underlying substrate. As a consequence the strain field in the substrate was calculated up to a depth equal to the island height and laterally up to three times the island base width. The use of larger sample volumes in the calculations has no further influence on the calculated strain field inside the island and its vicinity.

Based on atomic scatterers our approach seems to be not feasible because objects sizes larger then 20 nanometers will result in impracticable computing times. However, the smallest scatterer considered in the calculation may comprise a cell volume V_U (basic cell) that is much larger than an atom or even the crystallographic unit cell volume V_E. More precisely, we choose the basic cell such that (i) the atomic displacement changes $\Delta\mathbf{u}$ inside the basic cell are much smaller than an interatomic distance, and (ii) the associated basic cell shape function extends much further in reciprocal space than the area investigated in the experiment. Consequently, the basic cell volume V_U can be adapted depending on the size of the mesoscopic structures. We treat the deformation field $\mathbf{u}(\mathbf{r})$ as a smooth function over several basic cells, i.e., we neglect spatial frequencies of $\mathbf{u}(\mathbf{r})$ outside the area in reciprocal space that is investigated in the experiment.

In order to make interpretation of the results easier, we will shortly discuss the strain distribution inside an island with a homogeneous Ge content. In Fig. 3(a) the calculated elastic strain energy density ϵ in the (110) plane through the middle axis of a $Si_{0.75}Ge_{0.25}$ truncated pyramid is displayed. The overall amount of elastic strain energy is stored in the proximity of the island base edges aligned along $\langle 110\rangle$ whereas interfacial island regions close to the middle axis exhibit a reduced strain energy density. The upper part of the island is strongly relaxed and nearly free of elastic strain. This behavior is also illustrated in selected linescans for the strain tensor diagonal components (total strain[23]) $\varepsilon_{xx}(z)$ and $\varepsilon_{zz}(z)$ along the middle axis of the truncated pyramid [Fig. 3(b)], respectively, providing three important results: (i) $\varepsilon_{xx}(z)$ saturates at the top of the pyramid and, thus, substantially deviates from a power-law dependence[24] or a quadratic

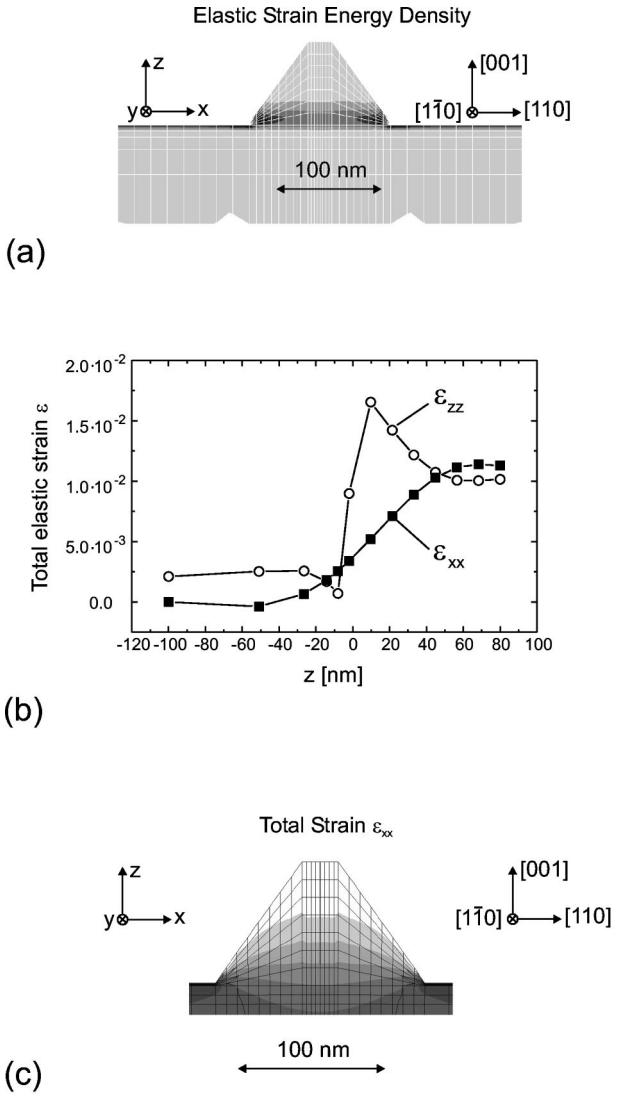

FIG. 3. Finite element calculation for a $Si_{0.75}Ge_{0.25}$ pyramid grown coherently on Si (001). (a) Elastic strain energy density ϵ in the (110) plane through the middle axis of the pyramid. The contour levels vary from 0 (bright) to $2.5\cdot 10^7$ J/m^3 (dark) on a linear scale. The thin white lines represent the used FEM mesh. (b) Total strain tensor components $\varepsilon_{zz}(z)$ and $\varepsilon_{xx}(z)$ along z axis (center of pyramid). $z=0$ denotes the interface between wetting layer and island. (c) Total strain tensor component $\varepsilon_{xx}(z)$ in the (110) plane through the middle axis of the pyramid. The contour levels vary from -4.2×10^{-3} (dark) to 1.4×10^{-2} (bright) on a linear scale.

expression used by Steinfort *et al.*[6] for Ge hut clusters on Si(001), (ii) $\varepsilon_{zz}(z)$ peaks at about $z=0$ and reaches complete relaxation at the upper half of the island, and (iii) there is strong penetration of $\varepsilon_{zz}(z)$ into the substrate. It should be noted that the strain energy seems to depend on the height only, at least far from the island edges. This does not hold for the strain parallel to the sample surface as is shown for ε_{xx} in Fig. 3(c).

Inside the island the FEM mesh size varies from 0.5 to 10 nm. Through linear inter-polation this mesh was transformed into a regular secondary mesh (''basic cells'') exhibiting a cell size of four times the Si lattice parameter ($a=5.43$ Å), which is still small enough such that no cell size effect substantially influences the calculated intensity distribution in

reciprocal space. In the framework of kinematical theory the diffracted intensity is given as a coherent sum of the scattering amplitudes from all atoms

$$I(\mathbf{q}) \propto \left| \sum_j f_j(\mathbf{q}) e^{i\mathbf{q}(\mathbf{r}_j + \mathbf{u}_j)} \right|^2, \tag{1}$$

where $f_j(\mathbf{q})$ is the atomic scattering factor and $\mathbf{q}$ the scattering vector. $\mathbf{r}_j$ and $\mathbf{u}_j$ are the position and the displacement of the jth atom inside the ideal reference lattice that is identical to the ideal substrate lattice. Equation (1) transforms into a summation over all basic cells V_U

$$I(\mathbf{q}) \propto \left| \sum_k \tilde{F}_k(\mathbf{q}) e^{i\mathbf{q}(\mathbf{r}_k + \mathbf{u}_k)} \right|^2, \tag{2}$$

where $\tilde{F}_k(\mathbf{q})$, $\mathbf{r}_k$ and $\mathbf{u}_k$ are the structure factor, the position and the displacement of the kth basic cell, respectively.

This is an hierarchical approach in that the structure factor of a single crystallographic unit cell is calculated atomistically as a function of the scattering vector. The result is used to calculate the structure factor $\tilde{F}_k(\mathbf{q})$ of a set of unit cells forming the basic cell V_U as used in Eq. (2). Up to this point, only an averaged lattice displacement is taken into account. The sum in Eq. (2) gives the structure factor of a single island. Coherent summation over several islands allows the simulation of the scattering of an island array with a large number of islands of arbitrary size and location.

The limited resolution perpendicular to the PSD was taken into account in our calculations by integrating intensities over an appropriate range of Δq_y.

It is a common problem in x-ray scattering to distinguish between strain, shape, composition, and spatial correlation. Although crystal truncation rods (CTR) basically represent a shape effect it has been demonstrated by Steinfort *et al.*[6] that they can be used to model the lateral strain field in Ge hut clusters. In the present work we do not perform a CTR analysis but focus on an entire two-dimensional intensity distribution in the proximity of a reciprocal lattice point. Neglecting the influence of the island shape a reciprocal space map is a special projection of the complex three-dimensional strain field. We would like to emphasize that a two-dimensional map still ''images'' to some extent the local interplay of strain and tilts and, thus, represents a characteristic fingerprint of the strain field far more than a single CTR scan.

V. RESULTS AND DISCUSSION

Figure 4 shows calculated reciprocal space maps in the proximity of the (a) 004 and (b) $\bar{1}13$ asymmetrical reciprocal lattice points[25] for an island exhibiting a constant Germanium concentration of $c = 25\%$. Island correlation effects were not considered in the calculation as will be discussed later. For 004 the intensity distribution consists of a rather sharp peak ($P1$), which is surrounded by a characteristic butterfly-shaped diffuse feature ($P2$). The features observed in the vicinity of 004 are also present in the asymmetrical case of $\bar{1}13$. We again observe a strong central peak ($P1$) that is embedded in strong diffuse intensity ($P2$). The peak

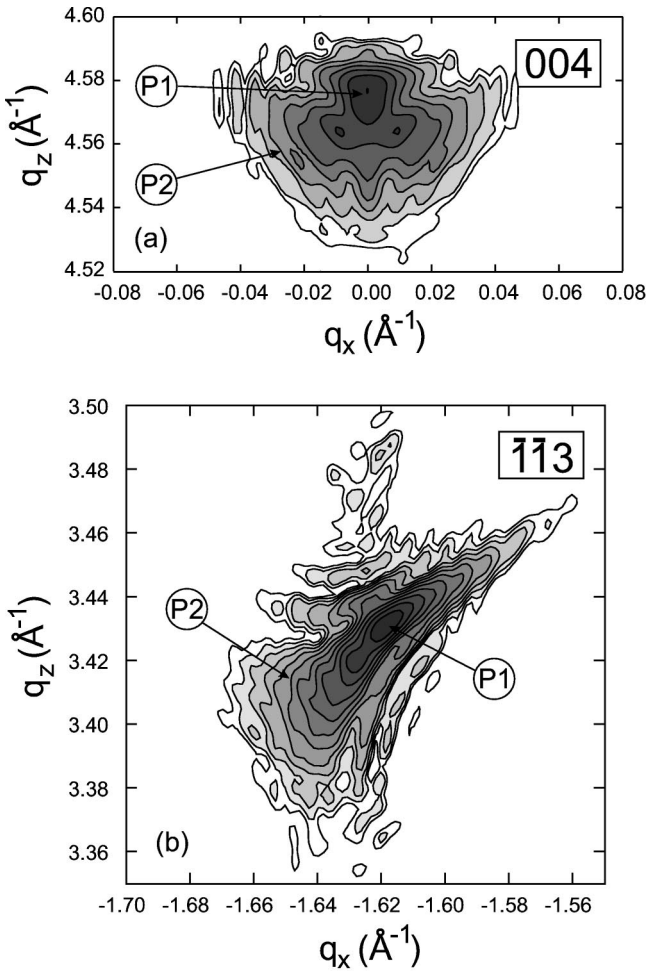

FIG. 4. X-ray intensity simulations for a homogeneous $Si_{0.75}Ge_{0.25}$ island in the vicinity of the (a) 004 and (b) $\bar{1}13$ reciprocal lattice points. The contour levels vary on a logarithmic scale within factors of $\sqrt{2}$.

position of $P1$ indicates cubic lattice symmetry and, thus, complete elastic relaxation.

A more detailed examination of our calculations shows that the origin of $P2$ are island sections close to the island-substrate interface whereas the central peak $P1$ is due to diffraction from the upper half of the island. This behavior is a direct consequence of the spatial strain distribution (Fig. 3), i.e., the island is nearly free of elastic strain in the upper part and highly strained close to the island-substrate interface.

We have investigated the characteristic shape of the butterfly $P2$ (of 004) by studying different azimuthal orientations of the sample with respect to the incoming beam. It is mainly influenced by the complex interplay of strain and local tilts of the atomic planes inside the island. In particular, we would like to point out that the wings of the butterfly *are not identical* with the {111} truncation rods of the islands, since they also appear—though differing in some detail—at island orientations with vanishing CTR's, e.g., incoming beam parallel to ⟨100⟩.

Note that, the two main features $P1$ and $P2$ are accompanied by weak thickness fringes that are due to the finite island height (80 nm). The 'bending' of the fringes indicate that they are sensitive to strain. A similar strain-induced deformation of characteristic features in reciprocal space has

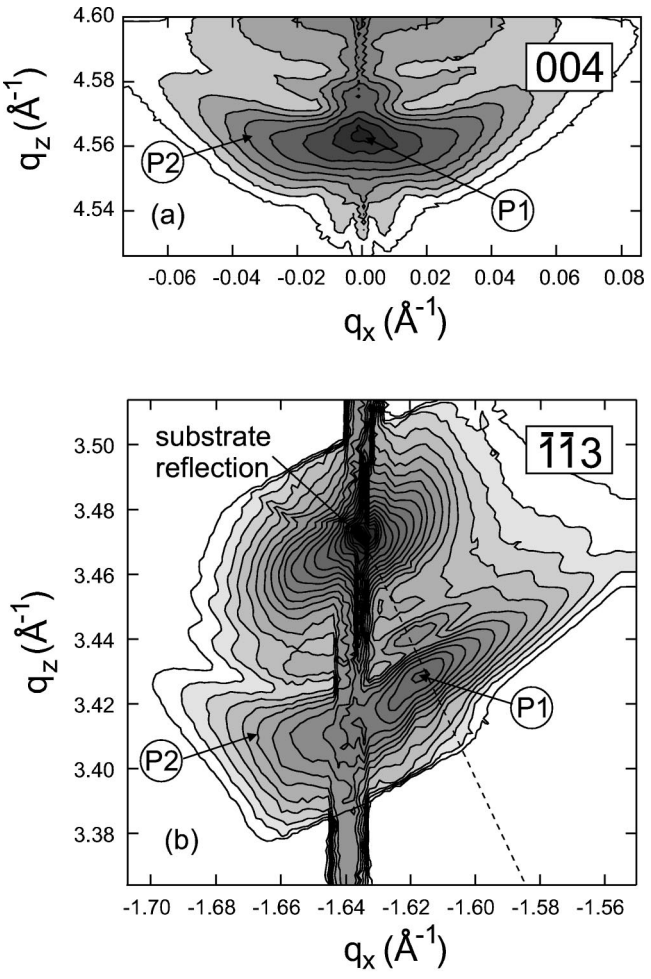

FIG. 5. Measured reciprocal space maps in the vicinity of (a) the 004 and (b) $\bar{1}\bar{1}3$ reciprocal lattice points. The contour levels vary on a logarithmic scale within factors of $\sqrt{2}$. For case (a) only the intensity due to the islands is displayed, whereas for (b) both the intensity due to the substrate and the SiGe layer is shown. The dashed line indicates areas with cubic lattice symmetry.

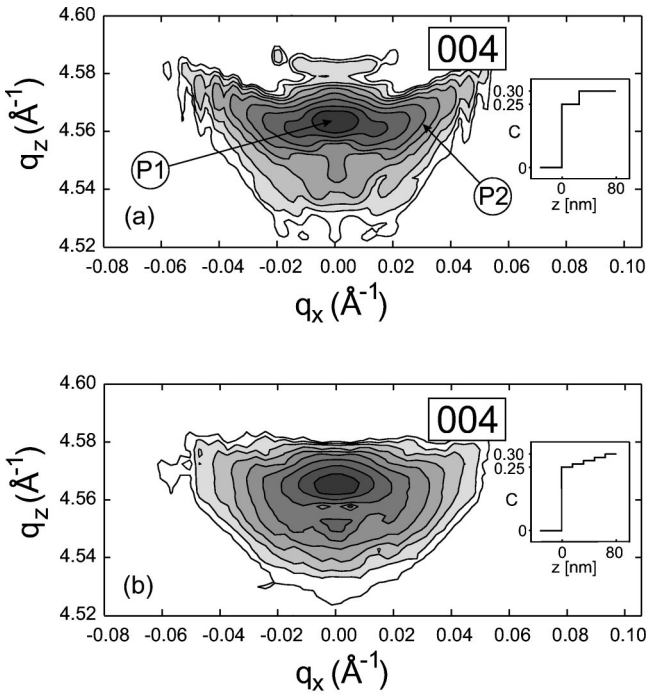

FIG. 6. X-ray intensity simulations in the vicinity of 004 for (a) an abrupt change of Ge composition at one third of the island height with $c_1=25\%$ in the lower part and $c_2=30\%$ in the upper part of the island, respectively (see insert). (b) Calculation using a linear increase of Ge composition with $c=25\%$ at the bottom and $c=30\%$ at the top of the island. The linear increase has been approximated by five layers of constant Ge concentration, as indicated in the insert. The contour levels vary on a logarithmic scale within factors of $\sqrt{2}$.

been found for quantum-wire structures.[16,17,24]

Our calculations were used to evaluate experimental scattering profiles. Figure 5 displays measured reciprocal space maps in the proximity of the (a) 004 and (b) $\bar{1}\bar{1}3$ reciprocal lattice points. Remarkable agreement between the respective experimental and simulated reciprocal space maps (Fig. 4) is obtained, i.e., (i) the intensity distribution of the layer reflection strongly extends in angular direction and, (ii) shows a rather sharp central peak $P1$, (iii) along with a butterfly-shaped feature ($P2$), which exhibits thickness fringes.

Complete agreement between the experimental data and the simulation for a homogeneous island is not evident since peak positions as well as respective peak widths, shapes and intensities are at variance with experiment. This can be improved by allowing for a variation of the Ge composition inside the island. In order to restrict the number of free parameters, a vertical composition profile is assumed, i.e., $c(z)$. First, the relative peak positions of $P1$ and $P2$ can be adjusted by introducing an increased value of $c=30\%$ at the top part of the island. This shifts the central peak $P1$ into the correct vertical q position (004: $q_z=4.56\,\text{Å}^{-1}$) and clearly better agreement between experiment and simulation is achieved. It turned out that the overall shape of the butterfly $P2$ is very sensitive to the functional dependence $c(z)$. Therefore, in a second step, various one-dimensional functions $c(z)$ have been checked as illustrated in Fig. 6 with two examples for the 004 reflection. Fig. 6(a) was calculated using an abrupt change of c at about one third of the island height with respective Ge concentrations of $c_1=25\%$ in the lower part and $c_2=30\%$ in the upper part of the island, whereas Fig. 6(b) shows the result of a linear increase $c(z)\sim z$ starting from $c_1=25\%$ at the bottom of the island up to $c_2=30\%$ at the top. This linear increase is approximated by five layers of constant Ge concentration [see insert of Fig. 6(b)].

Surprisingly, the abrupt change of $c(z)$ yields better agreement with the experimental results rather than a soft linear variation of $c(z)$ with z. This statement is underpinned by the following two points: (i) a soft gradient produces an extended intensity distribution along q_z, which is in clear contradiction to the comparably narrow distribution observed in experiment. Therefore, a rather steep function $c(z)$ is necessary. (ii) The ''wings'' of the butterfly that are clearly pronounced in experiment [Fig. 5(a)] are better reproduced for an abrupt Ge change.

The model of Fig. 6(a) was compared with similar ones, e.g., with the abrupt change at one fourth or one half of the island height or with a change of the Ge concentration in the lower or upper part of the island. Such slightly different models produce changes in the intensity distribution result-

ing in significantly worse correspondence with the experiment. Therefore, the accuracy of the position of the abrupt change is approximately $\pm 5\%$ of the island height and the accuracy of the Ge concentration is about $\pm 1\%$. Consequently, ''abrupt'' means an increase of the Ge concentration over a distance of about one tenth of the height or less.

However, characteristic differences seem to remain between experiment and simulation. Further work is necessary in order to clarify whether these differences are significant enough to allow for further refinement of the model, e.g., by replacing the one-dimensional variation of Ge concentration along z by a three dimensional distribution.

In this study a dispersion of the island sizes has not been taken into account. It proved practically negligible for the given narrow size distribution. This is due to the following reasons: First, as will be discussed below, the strain distribution inside the island does not depend on the island size. Therefore, the shape of diffuse scattering due to strain is also not substantially changed. Secondly, at the present island size the island shape function has no prevalent influence on the intensity distribution in reciprocal space. In other words: the diffuse scattering due to the finite size of the island is small.

From a previous investigation[13,14] we expect strong island-island correlation. This should lead to a modulation of strain-induced diffuse intensity parallel to the lateral scattering vector component q_x. However, we could not detect first-order correlation peaks (rods) in our experimental data. According to AFM data evaluation and grazing incidence small angle x-ray scattering[13] these should appear at about $\Delta q_x = \pm 3.10^{-3}\,\text{Å}^{-1}$. We cannot give a definite explanation why correlation is not visible in the present experiment. Since the x-ray coherence length is of the order of less than 4 μm the coherent signal originates from about 400 islands, which probably yields a small correlation signal only. This was also confirmed by calculations which explicitely took into account correlation by coherent summation of the scattering amplitudes of 400 islands ordered in an array according to the island positions in AFM images.

Finally, the applicability of our method will be discussed. We have reported on measurements and respective simulations on SiGe islands on the 100-nm scale. In that regime we observe size effects (thickness fringes) and strain effects, which yield a characteristic bending of the intensity distribution (''butterfly''). Can strain be also evaluated when going to smaller objects on a length scale of typically 30 nm (quantum dots) where the object shape function strongly extends into reciprocal space? For that purpose we will discuss the elastic equilibrium condition[26]

$$c_{ijkl}\left(\frac{\partial^2 \mu_k}{\partial x_j \partial x_l} - \alpha_{\mathrm{Ge}} \delta_{kl} \frac{\partial c}{\partial x_j}\right) + g_i(\mathbf{r}) = 0, \tag{3}$$

(using the Einstein sum rule) in more detail. Here, c_{ijkl} is the tensor of elastic moduli, c is the Germanium atomic fraction, α_{Ge} the relative change of the mean lattice parameter due to Germanium incorporation in linear approximation, and $\mathbf{g}(\mathbf{r})$ is the density of (external) body forces. In the case of $g_i = 0$ and neglecting surface tension in the boundary conditions, this relationship is invariant against any change of c_{ijkl}. Therefore, as already stated by Grundmann, Stier, and Bimberg,[27] the strain distribution does not depend on the island size. As an important consequence, the strain related distribution of diffuse intensity in reciprocal space is not a function of the object size, whereas, in contrast, the distribution of diffuse intensity that is related to size effects inversely scales with the island dimensions. This will lead to significantly reduced sensitivity to strain effects as soon as the size induced intensity distribution is more extended than that due to strain. At least for LPE-grown islands this is partially compensated for due to the observed relationship[20] $w \propto c^{-2.03}$ between the island base width w and the Ge concentration c. We have performed simulations of islands with an island base width of $w = 30$ nm and a respective height of $h = 18$ nm. In order to extract the influence of strain on the diffraction pattern we first have calculated the hypothetical case of a strain free Si island coherently linked to the Si substrate. For these calculations we have used a basic cell size of $a = 5.43$ Å. The resulting reciprocal space map [Fig. 7(a)] clearly shows (i) extended truncation rods due to the {111} and (001) facets, and (ii) thickness fringes due to the finite size of the island. When ''switching on'' strain (pure strained Ge) the intensity distribution changes to the well-known butterfly-shaped diffraction pattern, exhibiting, however, a remaining influence due to the thickness fringes [Fig. 7(b)]. The butterfly is more extended than the truncation rods

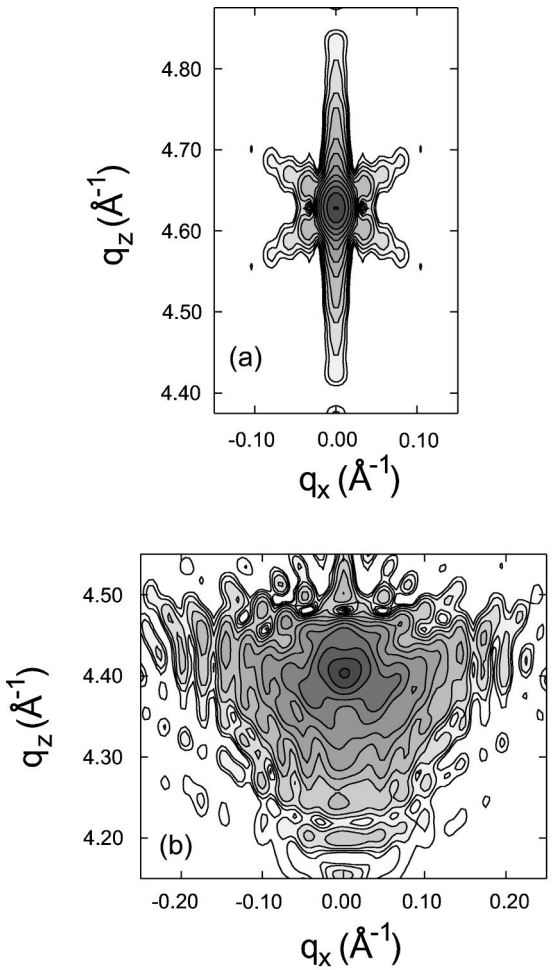

FIG. 7. Calculated diffraction pattern (004) for islands with width $w = 30$ nm and height $h = 18$ nm. (a) no strain and (b) pure Ge island on Si substrate. The contour levels differ by factors of $\sqrt{2}$.

of the unstrained Si islands so that we can conclude that the influence of strain on the intensity distribution is still prevalent.

Considering islands of constant area coverage the total volume per illuminated area of a two-dimensional island array is proportional to the island size. The extent of diffuse scattering due to size only inversely scales with size. Therefore, the local diffuse intensity in reciprocal space scales with the fourth power of size as soon as the size effect predominates. This is a serious problem for measurement at very small islands. Then it may prove necessary to make use of the diffuse scattering in the substrate reflection (or in the reflection of the host lattice in case of embedded islands).

As visible in Fig. 5(b) there is strong diffuse scattering near the substrate peak. This can be qualitatively understood since the strain field strongly extends into the substrate (see Fig. 3). Theoretical treatment of the substrate reflection requires a slightly modified approach because the kinematical approximation is inadequate for the perfect nonstrained part of the substrate. The diffuse intensity, however, can be easily implemented into the calculations by considering the difference of the electron densities of the strained crystal as compared to the perfect nonstrained matrix. The results of the simulation (Fig. 8) agree well with the experimental results [Fig. 5(b)]. It is maybe worthwhile to note that both experiment and simulation show a spiral-shaped intensity distribution.

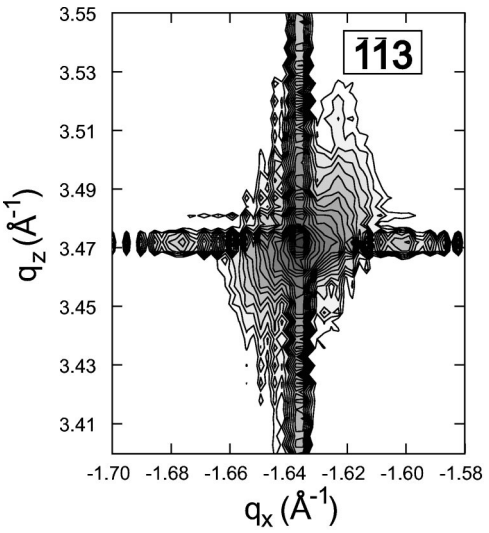

FIG. 8. Simulation of diffuse intensity around the $\bar{1}\bar{1}3$ substrate reflection. The horizontal streak is an artificial truncation rod due to the borders of the calculated area.

VI. CONCLUSIONS

We have demonstrated that the combined use of finite element calculations and a brute force kinematical scattering theory allows for the calculation of reciprocal space maps of strained nanoscale islands. The capabilities of this method, i.e., the comparison of theoretical simulations with measurements on highly regular coherent $Si_{0.75}Ge_{0.25}$ nanoscale islands grown on Si(001) is clearly illustrated. Good agreement is obtained by assuming a vertical Ge concentration gradient inside the islands. The applicability of our model to smaller islands such as quantum dots is also a distinct advantage.

ACKNOWLEDGMENTS

We have profited very much from extensive discussion with M. Albrecht and S. Christiansen (University of Erlangen, Germany). Critical reading of the manuscript by A. L. D. Kilcoyne (ALS, Berkeley, USA) is gratefully acknowledged. We thank I. Poppe (Paul-Drude-Institut, Berlin, Germany) for carrying out the SEM measurements. This work was supported within the framework of Sfb 296 of ''Deutsche Forschungsgemeinschaft,'' by ''Max-Planck-Gesellschaft'' and by ''Volkswagenstiftung'' (Contract No. I/71 181).

[1] I. N. Stranski and L. Krastanov, Akad. Wiss. Lit. Mainz Abh. Math. Naturwiss. Kl. **146**, 797 (1939).
[2] For an overview see the articles in MRS Bulletin 23 (1998).
[3] J. Tersoff, Phys. Rev. Lett. **81**, 3183 (1998).
[4] R. Bierwolf, M. Hohenstein, F. Philipp, O. Brandt, G. E. Crook, and K. Ploog, Ultramicroscopy **49**, 273 (1993); A. Rosenauer, S. Kaiser, T. Reisinger, J. Zweck, W. Gebhardt, and D. Gerthsen, Optik (Stuttgart) **102**, 63 (1996).
[5] S. Kret, T. Benabbas, C. Delamarre, Y. Androussi, A. Dubon, J. Y. Laval, and A. Lefebvre, J. Appl. Phys. **86**, 1988 (1999).
[6] A. J. Steinfort, P. M. L. O. Scholte, A. Ettema, F. Tuinstra, M. Nielsen, E. Landemark, D.-M. Smilgies, R. Feidenhans'l, G. Falkenberg, L. Seehofer, and R. L. Johnson, Phys. Rev. Lett. **77**, 2009 (1996).
[7] A. A. Darhuber, P. Schlittenhelm, V. Holý, J. Stangl, G. Bauer, and G. Abstreiter, Phys. Rev. B **55**, 15 652 (1997).
[8] A. A. Darhuber, V. Holý, J. Stangl, G. Bauer, A. Krost, F. Heinrichsdorff, M. Grundmann, D. Bimberg, V. M. Ustinov, P. S. Kop'ev, A. O. Kosogov, and P. Werner, Appl. Phys. Lett. **70**, 955 (1997).
[9] I. Kegel, T. H. Metzger, P. Fratzl, J. Peisl, A. Lorke, J. M. Garcia, and P. M. Petroff, Europhys. Lett. **45**, 222 (1999).
[10] I. Kegel, T. H. Metzger, J. Peisl, P. Schlittenhelm, and G. Abstreiter, Appl. Phys. Lett. **74**, 3978 (1999).
[11] V. Holý, J. Stangl, S. Zerlauth, G. Bauer, N. Darowski, D. Lübbert, and U. Pietsch, J. Phys. D **32**, A234 (1999).
[12] T. H. Metzger, I. Kegel, R. Paniago, and J. Peisl, J. Phys. D **32**, A202 (1999).
[13] M. Schmidbauer, Th. Wiebach, H. Raidt, M. Hanke, R. Köhler, and H. Wawra, Phys. Rev. B **58**, 10 523 (1998).
[14] M. Schmidbauer, Th. Wiebach, H. Raidt, M. Hanke, R. Köhler, and H. Wawra, J. Phys. D **32**, A230 (1999).
[15] S. Christiansen, M. Albrecht, H. P. Strunk, and H. J. Maier, Appl. Phys. Lett. **64**, 3617 (1994).
[16] Y. Zhuang, V. Holý, J. Stangl, A. A. Darhuber, P. Mikulik, S. Zerlauth, F. Schäffler, G. Bauer, N. Darowski, D. Lübbert, and U. Pietsch, J. Phys. D **32**, A224 (1999).
[17] G. T. Baumbach, D. Lübbert, and M. Gailhanou, J. Phys. D **32**,

A208 (1999).
[18] M. Grundmann and A. Krost (private communication).
[19] E. O. Kane, Phys. Rev. B **31**, 7865 (1985).
[20] W. Dorsch, H. P. Strunk, H. Wawra, G. Wagner, J. Groenen, and R. Carles, Appl. Phys. Lett. **72**, 179 (1998).
[21] S. R. Lee, B. L. Doyle, T. J. Drummond, J. W. Medernach, and R. P. Schneider, Jr, Adv. X-Ray Anal. **38**, 201 (1995).
[22] L. Vegard, Z. Phys. **5**, 17 (1921).
[23] In view of the way lattice parameter differences are handled in finite element calculations the total strain is used in the presentations, i.e., the Si substrate is used as reference every-where. Then a totally relaxed part of the island shows a total strain corresponding with the relative misfit between $Si_{1-c}Ge_c$ and the Si substrate.
[24] Q. Shen and S. Kycia, Phys. Rev. B **55**, 15 791 (1997); Q. Shen, S. W. Kycia, E. Tentarelli, W. Schaff, and L. F. Eastman, *ibid.* **54**, 16 381 (1996).
[25] Reciprocal space maps have been calculated with the in-plane component of the incoming beam collinear with ⟨110⟩.
[26] V. L. Indenbom and V. M. Kaganer, Phys. Status Solidi A **118**, 71 (1990); Equation (3) of this paper has been modified by introducing a composition gradient.
[27] M. Grundmann, O. Stier, and D. Bimberg, Phys. Rev. B **52**, 11 969 (1995).